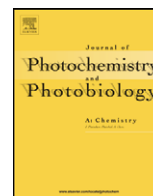




Contents lists available at ScienceDirect

# Journal of Photochemistry and Photobiology A: Chemistry

journal homepage: [www.elsevier.com/locate/jphotochem](http://www.elsevier.com/locate/jphotochem)

## Subject Index of Volume 200

### Absorption

Solvent dependent excited state spectral properties of 4-hydroxyacridine: Evidence for only water mediated excited state proton transfer process, 325

### Acceptor

Highly soluble perylene tetracarboxylic diimides and tetrathiafulvalene–perylene tetracarboxylic diimide–tetrathiafulvalene triads, 334

### Acrylamide polymers

Rhodamine-conjugated acrylamide polymers exhibiting selective fluorescence enhancement at specific temperature ranges, 432

### AFM

Surface properties and photocatalytic activity of nanocrystalline titania films, 192

### Aggregation

Photophysical behavior of lipophilic xanthene dyes without the involvement of photoinduced electron transfer mechanism, 307

### Alkaline hydrogen peroxide

Efficient total halogen-free photochemical bleaching of kraft pulps using alkaline hydrogen peroxide, 388

### Alkoxyxyanobiphenyls

Anomalous excimer formation of a pyrenyl derivative having a mesogen group of alkoxyxyanobiphenyl in its smectic mesophase, 232

### Alloxazine

Spectroscopy and photophysics of dimethyl-substituted alloxazines, 148

### Ammonia

The effect of Pt oxidation state and concentration on the photocatalytic removal of aqueous ammonia with Pt-modified titania, 246

Photocatalytic degradation of ammonia and butyric acid in plug-flow reactor: Degradation kinetic modeling with contribution of mass transfer, 254

### Anatase

Effect of pH and temperature on degradation of dilute dihydroxybenzene, in aqueous titanium dioxide suspension irradiated by UV light, 421

### Annealing

Effects of sintering of TiO<sub>2</sub> particles on the mechanisms of photocatalytic degradation of organic molecules in water, 216

### Annular reactor

Photocatalytic degradation of ammonia and butyric acid in plug-flow reactor: Degradation kinetic modeling with contribution of mass transfer, 254

### Anthracene

Host/guest complex of β-cyclodextrin/5-thia pentacene-14-one for photoinitiated polymerization of acrylamide in water, 377

### Avobenzene

Photostability of the sunscreens agent 4-*tert*-butyl-4'-methoxydibenzoylmethane (avobenzene) in solvents of different polarity and proticity, 410

### Azobenzene

Luminescence and structure of Eu(DBM)<sub>3</sub>Phen-doped vesicles composed of amphiphilic PNIPAM-*b*-PAzOM, 101

### Azoniaanthracene

The reversible [4 + 4] photocycloaddition of acridizinium derivatives, 3

### [1,1'-Binaphthalene]-2,2'-diol (1,1'-binaphthol or BINOL)

Fluorescence properties of (*R*)- and (*S*)-[1,1'-binaphthalene]-2,2'-diols solutions and their complexes with cyclodextrins in aqueous medium, 114

### Boron

Visible-light-driven boron/ferrum/cerium/titania photocatalyst, 141

### Bovine serum albumin

Photosensitizing properties of octacarboxy metallophthalocyanines in aqueous medium and their interaction with bovine serum albumin, 396

### Bridge groups

Structure and fluorescence properties of indole cyanine and merocyanine dyes with partially locked polymethine chain, 106

### Brij-35

Photoinduced electron transfer between quinones and amines in micellar media: Tuning the Marcus inversion region, 270

### Butyric acid

Photocatalytic degradation of ammonia and butyric acid in plug-flow reactor: Degradation kinetic modeling with contribution of mass transfer, 254

### Carbon nanotube

TiO<sub>2</sub>-carbon nanotube heterojunction arrays with a controllable thickness of TiO<sub>2</sub> layer and their first application in photocatalysis, 301

### Cerium

Visible-light-driven boron/ferrum/cerium/titania photocatalyst, 141

### Cetyltrimethylammonium bromide

Photoinduced electron transfer between quinones and amines in micellar media: Tuning the Marcus inversion region, 270

### Charge redistribution

Nanolayers of selected porphyrin and phthalocyanine dyes on solid substrates studied by electronic absorption and IR reflection–absorption spectroscopy, 225

### Chelating sulfoxide

Excited state isomerization in a new ruthenium chelating sulfoxide complex, 39

### Chemical liquid deposition

Room-temperature reaction of laser-photolytically generated Te nanosols with silver, 187

### Conformational analysis

Low temperature IR spectroscopy and photochemistry of matrix-isolated α-pyridil, 169

### Conjugate

Intramolecular energy transfer in rhodamine–phthalocyanine conjugates, 161

### π-Conjugated polymer

Triplet level-dependent photoluminescence and photoconduction properties of π-conjugated polymer thin films doped by iridium complexes, 371

### Crown ether

[2 + 2]-Photocycloaddition reaction of self-assembled crown-containing 2-styrylpyridinium perchlorate in a solid state, 90

### Crowned bis(spirobenzopyran)

Structural characterization for metal-ion complexation and isomerization of crowned bis(spirobenzopyran)s, 96

- Crystal structure  
Structural characterization for metal-ion complexation and isomerization of crowned bis(spirobenzopyran)s, 96
- Cyanine dyes  
Structure and fluorescence properties of indole cyanine and merocyanine dyes with partially locked polymethine chain, 106  
Fluorescence lifetime properties of near-infrared cyanine dyes in relation to their structures, 438
- Cyanuric acid  
Photo-induced transformation of hexaconazole and dimethomorph over TiO<sub>2</sub> suspension, 356
- β-Cyclodextrin  
Tuning the energy transfer process for the ensemble of fluorescein with β-cyclodextrin (β-CD) unit and spiroopyran with adamantyl (AD) unit: A temperature-gated molecular fluorescence switch, 83  
Host/guest complex of β-cyclodextrin/5-thia pentacene-14-one for photoinitiated polymerization of acrylamide in water, 377
- Cyclodextrins  
Fluorescence properties of (*R*)- and (*S*)-[1,1'-binaphthalene]-2,2'-diols solutions and their complexes with cyclodextrins in aqueous medium, 114
- Cyclohexyl alcohols  
Nanoparticles TiO<sub>2</sub>-photocatalyzed oxidation of selected cyclohexyl alcohols, 209
- Cypermethrin  
Photolysis of thin films of cypermethrin using in situ FTIR monitoring: Products, rates and quantum yields, 262
- Degradation  
Effects of sintering of TiO<sub>2</sub> particles on the mechanisms of photocatalytic degradation of organic molecules in water, 216
- Density Functional Theory (DFT)  
Solvent dependent excited state spectral properties of 4-hydroxyacridine: Evidence for only water mediated excited state proton transfer process, 325
- DFT  
Spectroscopy and photophysics of dimethyl-substituted alloxazines, 148
- DFT calculation  
Structural characterization for metal-ion complexation and isomerization of crowned bis(spirobenzopyran)s, 96
- DFT(B3LYP)/6-311++G(d,p) calculations  
Low temperature IR spectroscopy and photochemistry of matrix-isolated α-pyridil, 169
- Di- and tetrahydroindolizine (DHI, THI)  
Photochromism of dihydroindolizines. Part VIII. First holographic image recording based on di- and tetrahydroindolizines photochromes, 50
- Diarylethene  
Theoretical investigation on photochromic diarylethene: A short review, 10
- Diblock copolymer  
Luminescence and structure of Eu(DBM)<sub>3</sub>Phen-doped vesicles composed of amphiphilic PNIPAM-*b*-PAzOM, 101
- Dihydroindolizines (DHIs)  
Photochromism of dihydroindolizines Part IX. First attempts towards efficient self-assembling organogelators based on photochromic dihydroindolizines and *N*-acyl-1,ω-amino acid units, 57
- β-Diketone  
Synthesis and photophysical properties of novel organic-inorganic hybrid materials covalently linked to a europium complex, 318
- Dimethomorph  
Photo-induced transformation of hexaconazole and dimethomorph over TiO<sub>2</sub> suspension, 356
- Diphenyl ditelluride  
Room-temperature reaction of laser-photolytically generated Te nanosols with silver, 187
- 2,2-Diphenyl(2H)chromenes  
Structure effects on the photobehaviour of 2,2-diphenyl(2H)chromenes, 287
- Donor  
Highly soluble perylene tetracarboxylic diimides and tetrathiafulvalene-perylene tetracarboxylic diimide-tetrathiafulvalene triads, 334
- Dye-sensitized solar cells  
Photovoltaic performance of nanostructured zinc oxide sensitized with xanthene dyes, 364
- Dye-sensitized solar cell  
A module of a TiO<sub>2</sub> nanocrystalline dye-sensitized solar cell with effective dimensions, 314
- Electron paramagnetic resonance  
Production of reactive oxygen species induced by a new [60]fullerene derivative bearing a tetrazole unit and its possible biological applications, 277
- Electronic absorption  
Nanolayers of selected porphyrin and phthalocyanine dyes on solid substrates studied by electronic absorption and IR reflection-absorption spectroscopy, 225
- Electronic structure  
Structure and fluorescence properties of indole cyanine and merocyanine dyes with partially locked polymethine chain, 106
- Emission spectroscopy  
Excited state isomerization in a new ruthenium chelating sulfoxide complex, 39
- Energy transfer  
Triplet level-dependent photoluminescence and photoconduction properties of π-conjugated polymer thin films doped by iridium complexes, 371
- EPR  
Time-resolved EPR investigation on the photoreactions of vitamin K with antioxidant vitamins in micelle systems, 239
- ESIPT  
New 1,3,5-triphenyl-2-pyrazoline-containing 3-hydroxychromones as highly solvatofluorochromic ratiometric polarity probes, 426
- Europium complex  
Synthesis and photophysical properties of novel organic-inorganic hybrid materials covalently linked to a europium complex, 318
- Excimer fluorescence  
Anomalous excimer formation of a pyrenyl derivative having a mesogen group of alkoxyxanobiphenyl in its smectic mesophase, 232
- Excimer kinetics  
Anomalous excimer formation of a pyrenyl derivative having a mesogen group of alkoxyxanobiphenyl in its smectic mesophase, 232
- E-Z isomerization  
[2 + 2]-Photocycloaddition reaction of self-assembled crown-containing 2-styrylpyridinium perchlorate in a solid state, 90
- Ferrum  
Visible-light-driven boron/ferrum/cerium/titania photocatalyst, 141
- Flavins and flavoproteins  
Spectroscopic investigation of flavoproteins: Mechanistic differences between (electro)chemical and photochemical reduction and oxidation, 34
- Fluorescein  
Photophysical behavior of lipophilic xanthene dyes without the involvement of photoinduced electron transfer mechanism, 307
- Fluorescence  
Structure and fluorescence properties of indole cyanine and merocyanine dyes with partially locked polymethine chain, 106  
Fluorescence properties of (*R*)- and (*S*)-[1,1'-binaphthalene]-2,2'-diols solutions and their complexes with cyclodextrins in aqueous medium, 114  
Using hyperbranched macromers as crosslinkers of methacrylic networks prepared by photopolymerization, 126  
Spectroscopy and photophysics of dimethyl-substituted alloxazines, 148  
Photophysical behavior of lipophilic xanthene dyes without the involvement of photoinduced electron transfer mechanism, 307  
Solvent dependent excited state spectral properties of 4-hydroxyacridine: Evidence for only water mediated excited state proton transfer process, 325  
Rhodamine-conjugated acrylamide polymers exhibiting selective fluorescence enhancement at specific temperature ranges, 432  
UV-vis photodegradation of dyes in the presence of colloidal Q-CdS, 445

- Fluorescence imaging  
Multifunctional photo acid generator for fluorescence imaging based on self-contained photoreaction, 181
- Fluorescence lifetime  
Fluorescence lifetime properties of near-infrared cyanine dyes in relation to their structures, 438
- Fluorescence quantum yield  
Structure and fluorescence properties of indole cyanine and merocyanine dyes with partially locked polymethine chain, 106
- Fluorescence quenching  
Photosensitizing properties of octacarboxy metallophthalocyanines in aqueous medium and their interaction with bovine serum albumin, 396
- Fluorescence switch  
Tuning the energy transfer process for the ensemble of fluorescein with  $\beta$ -cyclodextrin ( $\beta$ -CD) unit and spiropyran with adamantyl (AD) unit: A temperature-gated molecular fluorescence switch, 83
- Fluorescent molecular probe  
Unusual fluorescence spectral response of 1-(4-*N,N*-dimethylamino-phenylethynyl)pyrene towards the thermotropic phase change in lipid bilayer membranes, 381
- Fluorescent sensor  
Effects of anionic surfactant SDS on the photophysical properties of two fluorescent molecular sensors, 402
- FT-IR reflection-absorption spectroscopy  
Nanolayers of selected porphyrin and phthalocyanine dyes on solid substrates studied by electronic absorption and IR reflection-absorption spectroscopy, 225
- FTIR spectroscopy  
Low temperature IR spectroscopy and photochemistry of matrix-isolated  $\alpha$ -pyridil, 169
- Fullerene C<sub>60</sub> derivative  
Production of reactive oxygen species induced by a new [60]fullerene derivative bearing a tetrazole unit and its possible biological applications, 277
- Fungicides  
Photo-induced transformation of hexaconazole and dimethomorph over TiO<sub>2</sub> suspension, 356
- Gated molecular switch  
Tuning the energy transfer process for the ensemble of fluorescein with  $\beta$ -cyclodextrin ( $\beta$ -CD) unit and spiropyran with adamantyl (AD) unit: A temperature-gated molecular fluorescence switch, 83
- Gelation  
Photochromism of dihydroindolizines Part IX. First attempts towards efficient self-assembling organogelators based on photochromic dihydroindolizines and *N*-acyl-1, $\omega$ -amino acid units, 57
- Hückel pyridine  
Low temperature IR spectroscopy and photochemistry of matrix-isolated  $\alpha$ -pyridil, 169
- Heterocycles  
A new family of photochromic compounds based on the photoinduced opening and thermal closing of [1,3]oxazine rings, 44
- Heterojunction  
TiO<sub>2</sub>-carbon nanotube heterojunction arrays with a controllable thickness of TiO<sub>2</sub> layer and their first application in photocatalysis, 301
- Hexaconazole  
Photo-induced transformation of hexaconazole and dimethomorph over TiO<sub>2</sub> suspension, 356
- Holographic data storage  
Photochromism of dihydroindolizines. Part VIII. First holographic image recording based on di- and tetrahydroindolizines photochromes, 50
- Holography  
Photochromism of dihydroindolizines. Part VIII. First holographic image recording based on di- and tetrahydroindolizines photochromes, 50
- Hybrid polyfunctional compounds  
Heading to photoswitchable magnets, 19
- Hydroquinone  
Effect of pH and temperature on degradation of dilute dihydroxybenzene, in aqueous titanium dioxide suspension irradiated by UV light, 421
- 4-Hydroxyacridine  
Solvent dependent excited state spectral properties of 4-hydroxyacridine: Evidence for only water mediated excited state proton transfer process, 325
- Hydroxyl radicals  
Surface properties and photocatalytic activity of nanocrystalline titania films, 192
- Hyperbranched macromers  
Using hyperbranched macromers as crosslinkers of methacrylic networks prepared by photopolymerization, 126
- Imidazolium  
Photophysical characterization of imidazolium-substituted Pd(II), In(III), and Zn(II) porphyrins as photosensitizers for photodynamic therapy, 346
- Inclusion complex  
Fluorescence properties of (*R*)- and (*S*)-[1,1'-binaphthalene]-2,2'-diols solutions and their complexes with cyclodextrins in aqueous medium, 114
- Intermolecular proton transfer  
Solvent dependent excited state spectral properties of 4-hydroxyacridine: Evidence for only water mediated excited state proton transfer process, 325
- Intramolecular energy transfer  
Intramolecular energy transfer in rhodamine-phthalocyanine conjugates, 161
- Isomerization  
Structural characterization for metal-ion complexation and isomerization of crowned bis(spirobenzopyran)s, 96
- Kinetic modeling  
Photocatalytic degradation of ammonia and butyric acid in plug-flow reactor: Degradation kinetic modeling with contribution of mass transfer, 254
- Kinetics  
Nanoparticles TiO<sub>2</sub>-photocatalyzed oxidation of selected cyclohexyl alcohols, 209
- Kraft pulp  
Efficient total halogen-free photochemical bleaching of kraft pulps using alkaline hydrogen peroxide, 388
- Langmuir-Hinshelwood  
Photocatalytic degradation of ammonia and butyric acid in plug-flow reactor: Degradation kinetic modeling with contribution of mass transfer, 254
- Lanthanide complex  
Luminescence and structure of Eu(DBM)<sub>3</sub>Phen-doped vesicles composed of amphiphilic PNIPAM-*b*-PAzoM, 101
- Laser flash photolysis  
A new family of photochromic compounds based on the photoinduced opening and thermal closing of [1,3]oxazine rings, 44
- Laser photolysis  
Room-temperature reaction of laser-photolytically generated Te nanosols with silver, 187
- Light scattering particle  
Influence of light scattering particles in the TiO<sub>2</sub> photoelectrode for solid-state dye-sensitized solar cell, 294
- Linkage isomerization  
Excited state isomerization in a new ruthenium chelating sulfoxide complex, 39
- Lipase  
Photophysical behavior of lipophilic xanthenes dyes without the involvement of photoinduced electron transfer mechanism, 307
- Lipid bilayer membrane  
Unusual fluorescence spectral response of 1-(4-*N,N*-dimethylamino-phenylethynyl)pyrene towards the thermotropic phase change in lipid bilayer membranes, 381
- Liquid crystals  
Anomalous excimer formation of a pyrenyl derivative having a mesogen group of alkoxyxanobiphenyl in its smectic mesophase, 232

- LOV domains  
Spectroscopic investigation of flavoproteins: Mechanistic differences between (electro)chemical and photochemical reduction and oxidation, 34
- Low temperature solid state  
Low temperature IR spectroscopy and photochemistry of matrix-isolated  $\alpha$ -pyridil, 169
- Lumazine  
Photochemical and photophysical properties of lumazine in aqueous solutions, 282
- Lumichrome  
Spectroscopy and photophysics of dimethyl-substituted alloxazines, 148
- Luminescence  
Luminescence and structure of  $\text{Eu}(\text{DBM})_3\text{Phen}$ -doped vesicles composed of amphiphilic PNIPAM-*b*-PAzoM, 101
- Magnetic properties  
Heading to photoswitchable magnets, 19
- Marcus inversion  
Photoinduced electron transfer between quinones and amines in micellar media: Tuning the Marcus inversion region, 270
- Mass transfer  
Photocatalytic degradation of ammonia and butyric acid in plug-flow reactor: Degradation kinetic modeling with contribution of mass transfer, 254
- Matrix isolation  
Low temperature IR spectroscopy and photochemistry of matrix-isolated  $\alpha$ -pyridil, 169
- Merocyanines  
Structure and fluorescence properties of indole cyanine and merocyanine dyes with partially locked polymethine chain, 106
- Mesophase  
Anomalous excimer formation of a pyrenyl derivative having a mesogen group of alkoxycyanobiphenyl in its smectic mesophase, 232
- Metal ion complex  
Structural characterization for metal-ion complexation and isomerization of crowned bis(spirobenzopyran)s, 96
- Micellar electron transfer  
Photoinduced electron transfer between quinones and amines in micellar media: Tuning the Marcus inversion region, 270
- Micelle  
Time-resolved EPR investigation on the photoreactions of vitamin K with antioxidant vitamins in micelle systems, 239  
Effects of anionic surfactant SDS on the photophysical properties of two fluorescent molecular sensors, 402
- Module  
A module of a  $\text{TiO}_2$  nanocrystalline dye-sensitized solar cell with effective dimensions, 314
- Molecular arrangement  
Nanolayers of selected porphyrin and phthalocyanine dyes on solid substrates studied by electronic absorption and IR reflection-absorption spectroscopy, 225
- Molecular mechanics  
Fluorescence properties of (*R*)- and (*S*)-[1,1'-binaphthalene]-2,2'-diols solutions and their complexes with cyclodextrins in aqueous medium, 114
- Molecular orbital  
Theoretical investigation on photochromic diarylethene: A short review, 10
- Molecular switches  
A new family of photochromic compounds based on the photoinduced opening and thermal closing of [1,3]oxazine rings, 44  
High-contrast fluorescence switching using a photoresponsive dithienylethene coordination compound, 74
- Morpholine  
Photo-induced transformation of hexaconazole and dimethomorph over  $\text{TiO}_2$  suspension, 356
- Multi-band fluorescence emission  
New 1,3,5-triphenyl-2-pyrazoline-containing 3-hydroxychromones as highly solvatofluorochromic ratiometric polarity probes, 426
- Multifunctional material  
Multifunctional photo acid generator for fluorescence imaging based on self-contained photoreaction, 181
- Nanoscience  
UV-vis photodegradation of dyes in the presence of colloidal Q-CdS, 445
- 1,8-Naphthalimide  
Multifunctional photo acid generator for fluorescence imaging based on self-contained photoreaction, 181
- Naphthopyran  
Photogeneration of an ADADA H-bonding cleft based on a naphthopyran-decorated triazine, 68
- Networks  
Using hyperbranched macromers as crosslinkers of methacrylic networks prepared by photopolymerization, 126
- Nitrogen heterocycles  
The reversible [4 + 4] photocycloaddition of acridizinium derivatives, 3
- NMR spectroscopy  
Photogeneration of an ADADA H-bonding cleft based on a naphthopyran-decorated triazine, 68
- OLED  
Triplet level-dependent photoluminescence and photoconduction properties of  $\pi$ -conjugated polymer thin films doped by iridium complexes, 371
- Orange II  
UV-vis photodegradation of dyes in the presence of colloidal Q-CdS, 445
- Organic dyes  
Photovoltaic performance of nanostructured zinc oxide sensitised with xanthene dyes, 364
- Organic-inorganic hybrid composite  
Synthesis and photophysical properties of novel organic-inorganic hybrid materials covalently linked to a europium complex, 318
- Oxazines  
A new family of photochromic compounds based on the photoinduced opening and thermal closing of [1,3]oxazine rings, 44
- Oxidation  
Effect of pH and temperature on degradation of dilute dihydroxybenzene, in aqueous titanium dioxide suspension irradiated by UV light, 421
- Oxidative process  
Efficient total halogen-free photochemical bleaching of kraft pulps using alkaline hydrogen peroxide, 388
- Partition coefficient  
Unusual fluorescence spectral response of 1-(4-*N,N*-dimethylamino-phenylethynyl)pyrene towards the thermotropic phase change in lipid bilayer membranes, 381
- Perylene tetracarboxylic diimide  
Highly soluble perylene tetracarboxylic diimides and tetrathiafulvalene-*perylene* tetracarboxylic diimide-tetrathiafulvalene triads, 334
- Pesticides  
Photolysis of thin films of cypermethrin using in situ FTIR monitoring: Products, rates and quantum yields, 262
- Phase transition  
Unusual fluorescence spectral response of 1-(4-*N,N*-dimethylamino-phenylethynyl)pyrene towards the thermotropic phase change in lipid bilayer membranes, 381
- 4 + 4 photocycloaddition  
The reversible [4 + 4] photocycloaddition of acridizinium derivatives, 3
- Phosphorescence  
Triplet level-dependent photoluminescence and photoconduction properties of  $\pi$ -conjugated polymer thin films doped by iridium complexes, 371
- Photoacid generator  
Multifunctional photo acid generator for fluorescence imaging based on self-contained photoreaction, 181
- Photocatalysis  
Surface properties and photocatalytic activity of nanocrystalline titania films, 192  
Nanoparticles  $\text{TiO}_2$ -photocatalyzed oxidation of selected cyclohexyl alcohols, 209  
Effects of sintering of  $\text{TiO}_2$  particles on the mechanisms of photocatalytic degradation of organic molecules in water, 216  
The effect of Pt oxidation state and concentration on the photocatalytic removal of aqueous ammonia with Pt-modified titania, 246

- Photocatalytic degradation of ammonia and butyric acid in plug-flow reactor:  
Degradation kinetic modeling with contribution of mass transfer, 254
- TiO<sub>2</sub>-carbon nanotube heterojunction arrays with a controllable thickness of TiO<sub>2</sub> layer and their first application in photocatalysis, 301
- Photo-induced transformation of hexaconazole and dimethomorph over TiO<sub>2</sub> suspension, 356
- Photocatalytic  
Effect of pH and temperature on degradation of dilute dihydroxybenzene, in aqueous titanium dioxide suspension irradiated by UV light, 421
- Photocatalytic oxidation  
Nanoparticles TiO<sub>2</sub>-photocatalyzed oxidation of selected cyclohexyl alcohols, 209
- Photochemical bleaching  
Efficient total halogen-free photochemical bleaching of kraft pulps using alkaline hydrogen peroxide, 388
- Photochemical reduction  
Spectroscopic investigation of flavoproteins: Mechanistic differences between (electro)chemical and photochemical reduction and oxidation, 34
- Photochemistry  
Spectroscopy and photophysics of dimethyl-substituted alloxazines, 148  
Low temperature IR spectroscopy and photochemistry of matrix-isolated  $\alpha$ -pyridil, 169
- Photochromic compounds  
Excited state isomerization in a new ruthenium chelating sulfoxide complex, 39
- Photochromic transformations  
Heading to photoswitchable magnets, 19
- Photochromism  
A new family of photochromic compounds based on the photoinduced opening and thermal closing of [1,3]oxazine rings, 44  
Photochromism of dihydroindolizines. Part VIII. First holographic image recording based on di- and tetrahydroindolizines photochromes, 50  
Photochromism of dihydroindolizines Part IX. First attempts towards efficient self-assembling organogelators based on photochromic dihydroindolizines and *N*-acyl-1, $\omega$ -amino acid units, 57  
Photogeneration of an ADADA H-bonding cleft based on a naphthopyran-decorated triazine, 68  
High-contrast fluorescence switching using a photoresponsive dithienylethene coordination compound, 74  
Structure effects on the photobehaviour of 2,2-diphenyl(2H)chromenes, 287
- Photocycloaddition  
[2 + 2]-Photocycloaddition reaction of self-assembled crown-containing 2-styrylpyridinium perchlorate in a solid state, 90
- Photocycloreversion  
The reversible [4 + 4] photocycloaddition of acridinium derivatives, 3
- Photodynamic therapy  
Photophysical characterization of imidazolium-substituted Pd(II), In(III), and Zn(II) porphyrins as photosensitizers for photodynamic therapy, 346
- Photoinduced electron transfer  
Multifunctional photo acid generator for fluorescence imaging based on self-contained photoreaction, 181  
Highly soluble perylene tetracarboxylic diimides and tetrathiafulvalene-perylene tetracarboxylic diimide-tetrathiafulvalene triads, 334
- Photokinetics  
Structure effects on the photobehaviour of 2,2-diphenyl(2H)chromenes, 287
- Photoluminescence  
Triplet level-dependent photoluminescence and photoconduction properties of  $\pi$ -conjugated polymer thin films doped by iridium complexes, 371
- Photolysis  
Time-resolved EPR investigation on the photoreactions of vitamin K with antioxidant vitamins in micelle systems, 239  
Photolysis of thin films of cypermethrin using in situ FTIR monitoring: Products, rates and quantum yields, 262
- Photooxidation  
Photolysis of thin films of cypermethrin using in situ FTIR monitoring: Products, rates and quantum yields, 262
- Photophysical property  
Synthesis and photophysical properties of novel organic-inorganic hybrid materials covalently linked to a europium complex, 318
- Photophysics  
Photophysical characterization of imidazolium-substituted Pd(II), In(III), and Zn(II) porphyrins as photosensitizers for photodynamic therapy, 346
- Photopolymerization  
Using hyperbranched macromers as crosslinkers of methacrylic networks prepared by photopolymerization, 126  
Host/guest complex of  $\beta$ -cyclodextrin/5-thia pentacene-14-one for photoinitiated polymerization of acrylamide in water, 377
- Photosensitizer  
Photophysical characterization of imidazolium-substituted Pd(II), In(III), and Zn(II) porphyrins as photosensitizers for photodynamic therapy, 346
- Photostability  
Photostability of the sunscreens agent 4-*tert*-butyl-4'-methoxydibenzoylmethane (avobenzene) in solvents of different polarity and proticity, 410
- Photoswitchable  
Photochromism of dihydroindolizines Part IX. First attempts towards efficient self-assembling organogelators based on photochromic dihydroindolizines and *N*-acyl-1, $\omega$ -amino acid units, 57
- Photovoltaic  
A module of a TiO<sub>2</sub> nanocrystalline dye-sensitized solar cell with effective dimensions, 314
- Phthalocyanine  
Intramolecular energy transfer in rhodamine-phthalocyanine conjugates, 161  
Photosensitizing properties of octacarboxy metallophthalocyanines in aqueous medium and their interaction with bovine serum albumin, 396
- Phthalocyanine Langmuir-Blodgett layers  
Nanolayers of selected porphyrin and phthalocyanine dyes on solid substrates studied by electronic absorption and IR reflection-absorption spectroscopy, 225
- Platinum  
The effect of Pt oxidation state and concentration on the photocatalytic removal of aqueous ammonia with Pt-modified titania, 246
- Polymer beads  
Influence of light scattering particles in the TiO<sub>2</sub> photoelectrode for solid-state dye-sensitized solar cell, 294
- Polymer vesicle  
Luminescence and structure of Eu(DBM)<sub>3</sub>Phen-doped vesicles composed of amphiphilic PNIPAM-*b*-PAzoM, 101
- Porphyrin  
Nanolayers of selected porphyrin and phthalocyanine dyes on solid substrates studied by electronic absorption and IR reflection-absorption spectroscopy, 225  
Photophysical characterization of imidazolium-substituted Pd(II), In(III), and Zn(II) porphyrins as photosensitizers for photodynamic therapy, 346
- Positive and negative holography  
Photochromism of dihydroindolizines. Part VIII. First holographic image recording based on di- and tetrahydroindolizines photochromes, 50
- Premicelle  
Effects of anionic surfactant SDS on the photophysical properties of two fluorescent molecular sensors, 402
- Protein electron transfer  
Spectroscopic investigation of flavoproteins: Mechanistic differences between (electro)chemical and photochemical reduction and oxidation, 34
- Pyrenyl compounds  
Anomalous excimer formation of a pyrenyl derivative having a mesogen group of alkoxy cyanobiphenyl in its smectic mesophase, 232
- $\alpha$ -Pyridil  
Low temperature IR spectroscopy and photochemistry of matrix-isolated  $\alpha$ -pyridil, 169
- Q-CdS  
UV-vis photodegradation of dyes in the presence of colloidal Q-CdS, 445
- Quinone  
Photoinduced electron transfer between quinones and amines in micellar media: Tuning the Marcus inversion region, 270
- Ratiometric probe  
New 1,3,5-triphenyl-2-pyrazoline-containing 3-hydroxychromones as highly solvatofluorochromic ratiometric polarity probes, 426



- Reactive oxygen species  
 Production of reactive oxygen species induced by a new [60]fullerene derivative bearing a tetrazole unit and its possible biological applications, 277
- Renewable energy  
 A module of a TiO<sub>2</sub> nanocrystalline dye-sensitized solar cell with effective dimensions, 314
- Rhodamine  
 Intramolecular energy transfer in rhodamine-phthalocyanine conjugates, 161  
 Rhodamine-conjugated acrylamide polymers exhibiting selective fluorescence enhancement at specific temperature ranges, 432
- Rotamers  
 Photogeneration of an ADADA H-bonding cleft based on a naphthopyran-decorated triazine, 68
- Ruthenium  
 Excited state isomerization in a new ruthenium chelating sulfoxide complex, 39
- Safranin-O  
 UV-vis photodegradation of dyes in the presence of colloidal Q-CdS, 445
- SDS  
 Effects of anionic surfactant SDS on the photophysical properties of two fluorescent molecular sensors, 402
- Self-assembly  
 Photochromism of dihydroindolizines Part IX. First attempts towards efficient self-assembling organogelators based on photochromic dihydroindolizines and *N*-acyl-1,ω-amino acid units, 57  
 [2 + 2]-Photocycloaddition reaction of self-assembled crown-containing 2-styrylpyridinium perchlorate in a solid state, 90  
 Using hyperbranched macromers as crosslinkers of methacrylic networks prepared by photopolymerization, 126
- Silver telluride films  
 Room-temperature reaction of laser-photolytically generated Te nanosols with silver, 187
- Singlet oxygen  
 Spectroscopy and photophysics of dimethyl-substituted alloxazines, 148  
 Photochemical and photophysical properties of lumazine in aqueous solutions, 282  
 Host/guest complex of β-cyclodextrin/5-thia pentacene-14-one for photoinitiated polymerization of acrylamide in water, 377
- Solar cell  
 A module of a TiO<sub>2</sub> nanocrystalline dye-sensitized solar cell with effective dimensions, 314
- Solid-state dye-sensitized solar cell  
 Influence of light scattering particles in the TiO<sub>2</sub> photoelectrode for solid-state dye-sensitized solar cell, 294
- Solid-state photochemistry  
 The reversible [4 + 4] photocycloaddition of acridinium derivatives, 3
- Solvatofluorochromism  
 Structure and fluorescence properties of indole cyanine and merocyanine dyes with partially locked polymethine chain, 106  
 New 1,3,5-triphenyl-2-pyrazoline-containing 3-hydroxychromones as highly solvatofluorochromic ratiometric polarity probes, 426
- Solvent polarity and proticity  
 Photostability of the sunscreens agent 4-*tert*-butyl-4'-methoxydibenzoylmethane (avobenzone) in solvents of different polarity and proticity, 410
- Spectroelectrochemistry  
 Spectroscopic investigation of flavoproteins: Mechanistic differences between (electro)chemical and photochemical reduction and oxidation, 34
- Spiropyran  
 Tuning the energy transfer process for the ensemble of fluorescein with β-cyclodextrin (β-CD) unit and spirocyan with adamantyl (AD) unit: A temperature-gated molecular fluorescence switch, 83
- Stern-Volmer  
 Photosensitizing properties of octacarboxy metallophthalocyanines in aqueous medium and their interaction with bovine serum albumin, 396
- Styrylpyridinium salt  
 [2 + 2]-Photocycloaddition reaction of self-assembled crown-containing 2-styrylpyridinium perchlorate in a solid state, 90
- Super-gels  
 Photochromism of dihydroindolizines Part IX. First attempts towards efficient self-assembling organogelators based on photochromic dihydroindolizines and *N*-acyl-1,ω-amino acid units, 57
- Te nanosols  
 Room-temperature reaction of laser-photolytically generated Te nanosols with silver, 187
- Temperature sensor  
 Rhodamine-conjugated acrylamide polymers exhibiting selective fluorescence enhancement at specific temperature ranges, 432
- Tetrathiafulvalene  
 Highly soluble perylene tetracarboxylic diimides and tetrathiafulvalene-perylene tetracarboxylic diimide-tetrathiafulvalene triads, 334
- Thermal bleaching  
 Structure effects on the photobehaviour of 2,2-diphenyl(2H)chromenes, 287
- Thioxanthone  
 Host/guest complex of β-cyclodextrin/5-thia pentacene-14-one for photoinitiated polymerization of acrylamide in water, 377
- TiO<sub>2</sub>  
 TiO<sub>2</sub>-carbon nanotube heterojunction arrays with a controllable thickness of TiO<sub>2</sub> layer and their first application in photocatalysis, 301  
 Photo-induced transformation of hexaconazole and dimethomorph over TiO<sub>2</sub> suspension, 356
- TiO<sub>2</sub> films  
 Surface properties and photocatalytic activity of nanocrystalline titania films, 192
- TiO<sub>2</sub> nanoparticles  
 Nanoparticles TiO<sub>2</sub>-photocatalyzed oxidation of selected cyclohexyl alcohols, 209
- Titania  
 Visible-light-driven boron/ferrum/cerium/titania photocatalyst, 141  
 The effect of Pt oxidation state and concentration on the photocatalytic removal of aqueous ammonia with Pt-modified titania, 246
- Titanium dioxide  
 Effects of sintering of TiO<sub>2</sub> particles on the mechanisms of photocatalytic degradation of organic molecules in water, 216
- Total halogen-free process  
 Efficient total halogen-free photochemical bleaching of kraft pulps using alkaline hydrogen peroxide, 388
- Transient spectra  
 Spectroscopy and photophysics of dimethyl-substituted alloxazines, 148
- Triazine  
 Photogeneration of an ADADA H-bonding cleft based on a naphthopyran-decorated triazine, 68
- 1,3,5-Triphenyl-2-pyrazoline-substituted 3-hydroxychromone  
 New 1,3,5-triphenyl-2-pyrazoline-containing 3-hydroxychromones as highly solvatofluorochromic ratiometric polarity probes, 426
- Triplet lifetime  
 Photosensitizing properties of octacarboxy metallophthalocyanines in aqueous medium and their interaction with bovine serum albumin, 396
- Triplet yield  
 Photosensitizing properties of octacarboxy metallophthalocyanines in aqueous medium and their interaction with bovine serum albumin, 396
- Triton-X-100  
 Photoinduced electron transfer between quinones and amines in micellar media: Tuning the Marcus inversion region, 270
- UV-A  
 Photochemical and photophysical properties of lumazine in aqueous solutions, 282

- Visible light photocatalysis
  - Visible-light-driven boron/ferrum/cerium/titania photocatalyst, 141
- Vitamin C
  - Time-resolved EPR investigation on the photoreactions of vitamin K with antioxidant vitamins in micelle systems, 239
- Vitamin K
  - Time-resolved EPR investigation on the photoreactions of vitamin K with antioxidant vitamins in micelle systems, 239
- Wastewater
  - Effect of pH and temperature on degradation of dilute dihydroxybenzene, in aqueous titanium dioxide suspension irradiated by UV light, 421
- Xanthene
  - Photovoltaic performance of nanostructured zinc oxide sensitised with xanthene dyes, 364
- Xanthene dye
  - Photophysical behavior of lipophilic xanthene dyes without the involvement of photoinduced electron transfer mechanism, 307
- XPS
  - Surface properties and photocatalytic activity of nanocrystalline titania films, 192
- ZnO nanoparticles
  - Photovoltaic performance of nanostructured zinc oxide sensitised with xanthene dyes, 364